Hernández Jiménez, V. J., Castronuovo, E. D. & Rodríguez-Morcillo, I. S. (2018). Optimal statistical calculation of underground cable bundles positions for time-varying currents. *International Journal of Electrical Power & Energy Systems, 95*, 26–35.

DOI: 10.1016/j.ijepes.2017.08.003

Optimal Statistical Calculation of Underground Cable Bundles Positions for Time-Varying Currents

Víctor J. Hernández Jiménez[1,2], Edgardo D. Castronuovo[1*], Ismael Sánchez Rodríguez-Morcillo[1,3]

[1]University Carlos III de Madrid, Avda. de la Universidad, 30, 28911 Leganés, Madrid, Spain
[2]Red Eléctrica de España, Pº Conde de los Gaitanes, 177, 28109 Alcobendas, Madrid, Spain
[3]Universidad de Piura, Avda. Ramón Múgica, 131, Urb. San Eduardo, Piura, Peru.
[*] ecastron@ing.uc3m.es (ORCID: 0000-0003-2292-4928)

Abstract. Underground cables are intensively used, especially for transporting energy in urban areas. In general, the currents flowing in the cables change, following the loads profile. Moreover, the optimal installation of these cables must consider geometry, magnetic fields and arrangement costs. This paper proposes and analyses different statistical calculations of these optimal locations. The application of the methods to real data demonstrates the effectiveness of the statistical approaches in terms of costs and magnetic fields.

Keywords. Magnetic fields; Underground cables; Optimization; Distribution grids.

1. Introduction

Underground cables currently transmit a huge amount of electrical energy in urban environments. Additionally, underground cables are increasingly used in transmission lines when particular landing characteristics motivate their utilization instead of using overhead power lines. As with any other electrical line, underground cables produce magnetic fields, which must be restricted in the interest of the population. The limits on maximum magnetic fields vary between countries and regions for the industrial frequency of 50/60 Hz. In 2010, the International Commission on Non-Ionizing Radiation Protection (ICNRP) recommended a maximum value of magnetic fields for general public exposure of 200 μT [1]. This large limit is different in certain countries. In the USA, a federal normative has not been introduced yet; however, some states, such as Florida (15 μT for up to 230 kV and 20 μT for higher voltages) and New York (20 μT), have introduced magnetic field limits [2]. In Europe, a maximum magnetic field of 100 μT is recommended, [3]. Although most European countries follow this recommendation, some countries have settled on stronger restrictions: in Belgium, the maximum value is 10 μT (Flanders region); in Italy, it is 3 or 10 μT (for new or existing installations); in Poland, it is 75 μT; and in Slovenia, it is 10 μT. Russia specified a maximum value of 10 μT, and Switzerland settled on a very small value of 1 μT [4], [5].

Edgardo Castronuovo acknowledges the Ministry of Science and Technology of Spain (Project RESMART. 2014/00338/001).

In [6], more than 140 papers are reviewed and discussed, therein summarizing possible techniques for mitigating extremely-low-frequency magnetic fields in transmission lines, focusing on overhead power lines. In [7], a new method for estimating the magnetic field generated by overhead transmission lines is also proposed, using hybrid genetic algorithms. Calculation methods for obtaining the optimal configuration of underground transmission lines are also present in the literature. The reduction in magnetic fields produced by underground cables is an increasingly popular research field with interesting practical applications. A multi-circuit underground cable system with unbalanced loads is analysed in [8]. The proposed algorithm finds the optimal configuration of an arrangement, therein selecting between specified locations of the cables. The reduction in magnetic field in a measurement plane 1 m above ground is searched in [9] for arrangements of 2, 3 and 4 three-phase systems. The optimal phase disposition of the currents is calculated, therein shifting the currents between fixed available positions. In [10], the possibility of twisting the cables is studied, which reduces the magnetic fields in the ground. In [11], [12] and [13], different shielding solutions are proposed for fixed-position underground cables. In [14], the junction tower with underground three-phase double circuits is analyzed, calculating the contour of the geometrical fields distributions.

In previous references, cable positions were fixed. In some of the studies, currents are allocated to pre-specified cable positions to search for the optimal phase configuration that reduces the magnetic field in a measurement plane. For shifting between positions, integer variables are generally used in the formulations, thus increasing the difficulty of the problem (in [15], a genetic algorithm is utilized to solve the optimization problem). In [16], a new formulation with all continuous variables is proposed in an attempt to calculate the optimal position of the underground cables. The algorithm obtains optimal positions and phase dispositions of the cables, therein searching for the minimization of construction costs. In this and previous studies, optimal dispositions of cable arrangements are calculated for specific values of currents. However, the currents in the cables change according to the load variations. In [17], multiple-circuit underground cable feeders with randomly varying loads are studied. The load current in all feeder circuits is considered as normally distributed. The optimal phase arrangement of the currents in a set of selected positions is calculated using a genetic algorithm. The authors conclude that the statistical approach results in better arrangements than when considering only a single value of current.

The main contributions of present proposal are: a) the use of statistical methods, based on resampling from real multivariate data, to obtain the optimal disposition of cables; b) the proposition of optimization methods with all continuous variables to calculate the optimal positions of the cables; c) the consideration of construction costs to calculate optimal dispositions, besides geometrical, constructive and magnetic field restrictions; and d) the evaluation of economic benefits related with rotated dispositions of cable bundles. Two new algorithms are proposed and compared, for calculating the optimal geometry and phase disposition of underground cables with time variating currents. The results show that the proposed statistical approach provides less expensive configurations and results in smaller magnetic fields than the conventional approach.

2. The optimization problems

In the present work, the objective is to determine the optimal coordinates for underground cables arranged in 3-phase cable bundles to achieve minimum possible construction costs and magnetic fields generated by time-varying currents flowing through n circuits. The optimization formulation is proposed for a general number of circuits. In the following, the two optimization problems solved in this work are described.

2.1. Minimization of costs and magnetic field generated by n-cable bundles with specified currents

The objective of the first optimization problem is to calculate the optimal coordinates of a set of underground cables arranged in n 3-phase cable bundles such that the minimum construction cost is attained. The calculation is performed for a specified maximum magnetic field in a measurement plane created by previously known fixed currents. Two types of solutions can be obtained: a) the case where cables at the position resulting in the minimum construction cost (as allowed by geometrical constraints) generate less than the maximum allowed magnetic field in the measurement plane and b) the case where the cables must be allocated to a more costly position to fulfil the magnetic field constraints. In the first case, the optimization problem seeks to calculate the optimal arrangement that reduces the maximum value of the maximum magnetic field in the measurement plane. In case b), the optimization problem obtains the minimum cost positions for the specified magnetic field conditions. The proposed optimization problem has the advantage that it can be used for any limit of maximum magnetic field, easily integrating the two different goals.

For specified currents in the cables and a maximum magnetic field allowed in the measurement plane, the proposed optimization problem can be summarized using equations (1)-(14).

$$\min f\left(x,y,\Delta B_{max}\right)= c_x \frac{\sum_{i=1}^{n}\left|x_i\right|}{n} - c_y y_1 - c_{vol} y_1 \frac{\sum_{i=1}^{n}\left|x_i\right|}{n} - Kp\ \Delta B_{max} \tag{1}$$

s.t.

$$b_x^{\,k}=\frac{\mu_0}{2\pi}\left|\begin{pmatrix} I_{1a}\dfrac{y_{1a}-Y_c}{\left(X_c-x_{1a}\right)^2+\left(Y_c-y_{1a}\right)^2}+I_{1b}\dfrac{y_{1b}-Y_c}{\left(X_c-x_{1b}\right)^2+\left(Y_c-y_{1b}\right)^2}+I_{1c}\cdot\dfrac{y_{1c}-Y_c}{\left(X_c-x_{1c}\right)^2+\left(Y_c-y_{1c}\right)^2}+\ldots \\ +I_{na}\dfrac{y_{na}-Y_c}{\left(X_c-x_{na}\right)^2+\left(Y_c-y_{na}\right)^2}+I_{nb}\dfrac{y_{nb}-Y_c}{\left(X_c-x_{nb}\right)^2+\left(Y_c-y_{nb}\right)^2}+I_{nc}\cdot\dfrac{y_{nc}-Y_c}{\left(X_c-x_{nc}\right)^2+\left(Y_c-y_{nc}\right)^2}\end{pmatrix}\right| \tag{2}$$

$$b_y^{\,k}=\frac{\mu_0}{2\pi}\left|\begin{pmatrix} I_{1a}\dfrac{X_c-x_{1a}}{\left(X_c-x_{1a}\right)^2+\left(Y_c-y_{1a}\right)^2}+I_{1b}\dfrac{X_c-x_{1b}}{\left(X_c-x_{1b}\right)^2+\left(Y_c-y_{1b}\right)^2}+I_{1c}\dfrac{X_c-x_{1c}}{\left(X_c-x_{1c}\right)^2+\left(Y_c-y_{1c}\right)^2}+\ldots \\ +I_{na}\dfrac{X_c-x_{na}}{\left(X_c-x_{na}\right)^2+\left(Y_c-y_{na}\right)^2}+I_{nb}\dfrac{X_c-x_{nb}}{\left(X_c-x_{nb}\right)^2+\left(Y_c-y_{nb}\right)^2}+I_{nc}\dfrac{X_c-x_{nc}}{\left(X_c-x_{nc}\right)^2+\left(Y_c-y_{nc}\right)^2}\end{pmatrix}\right| \tag{3}$$

$$\left(b_x^{\,k}\right)^2+\left(b_y^{\,k}\right)^2 \le B_{max}^2-\Delta B_{\max}^2 \tag{4}$$

$$\left(x_{ia}-x_{ib}\right)^2+\left(y_{ia}-y_{ib}\right)^2=d^2 \tag{5}$$

$$\left(x_{ia}-x_{ic}\right)^2+\left(y_{ia}-y_{ic}\right)^2=d^2 \tag{6}$$

$$\left(x_{ib}-x_{ic}\right)^2+\left(y_{ib}-y_{ic}\right)^2=d^2 \tag{7}$$

$$\frac{x_{ia}+x_{ib}+x_{ic}}{3}=x_i \tag{8}$$

$$\frac{y_{ia}+y_{ib}+y_{ic}}{3}=y_i \tag{9}$$

$$\Delta B_{\max}>0 \tag{10}$$

$$\left(x_i-x_j\right)^2+\left(y_i-y_j\right)^2 \ge d_{Min}^{\;2},\ i\ne j \tag{11}$$

$$y_1 \le y_i \tag{12}$$

$$-X_{Max}\le x_i \le X_{Max} \tag{13}$$

$$-Y_{Max}\le y_i \le -Y_{Min} \tag{14}$$

$$i,j=1,\ldots,n,\ \ k=1,\ \ldots,\ k_{Max}$$

where b_x^k and b_y^k are the modules of phasors of the horizontal and vertical components of the magnetic field at point k of the evaluation plane, in μT; (x_i,y_i) are the coordinates of the centre of the bundle of cables i, in m; (x_{il},y_{il}) are the coordinates of the centre of cable l in the bundle of cables i, in m; and ΔB_{Max} is the complementary variable measuring the difference between the maximum magnetic field allowed B_{Max} and the real maximum magnetic field observed in the evaluation plane. The constraints are as follows: μ_0 is the permeability of free space, in H m^{-1}; I_{il} is the phasor of currents flowing through the bundle of cables i, phases $l=\{a, b, c\}$, in A; b is the magnetic field, in μT; b_{xi} and b_{yi} are horizontal and vertical projections, respectively, of the magnetic field phasors generated by cable i, in μT; B_{Max} is the maximum magnetic field allowed in the evaluation plane, in μT; d is the distance between two centres of cables in a bundle, in m;

X_{Max} is the maximum horizontal distance allowed from the centre of a bundle and the horizontal reference, in m; and Y_{Max} and Y_{Min} are the maximum and minimum depth, respectively, allowed to the centre of any 3-phase cable bundle, in m.

The main costs associated with the installation of underground transmission lines are related to the civil construction and the right-of-path costs. Civil construction costs include expenses for digging plus filling and compacting the rectangular trench in which bundles are laid. Moreover, for security reasons and to prevent the possible collapse of the walls of the trench, it is necessary to shore up the walls during installation, which incurs additional costs. The right-of-path costs are associated with the occupation of the space.

Objective function (1) contains four terms. The firsts three terms consider the following: horizontal costs per unit associated with the occupation of the land (c_x), vertical costs per unit related to digging operations (c_y) and volumetric costs per unit due to movements of terrain (c_{vol}). Because the depth (y_i) is a negative variable, the second and third term are negative expressions. The first three terms of (1), therefore, attempt to reduce civil construction and right-of-path costs. The relationship between these costs will affect the shape of the solutions. Larger vertical costs will result in more superficial disposition of the cables. On the other hand, if horizontal costs are larger than vertical ones, cables will be allocated near vertical axis (Fig. 1.a). Volumetric costs lead to more concentrated solutions.

When the magnetic fields allowed in the measurement plane are relatively large, cables can adopt the minimum cost positions allowed by construction restrictions. In this case, the fourth term of (1) attempts to minimize the maximum magnetic field in the measurement plane, thereby increasing the complementary variable ΔB_{Max}. This additional variable reduces the maximum magnetic field allowed in the evaluation plane, when the cables can adopt minimum cost positions (see (4)). The penalty coefficient Kp is a small value and is lower than the costs in the first three terms of (1).

In (2) and (3), the modules of the phasors of the horizontal and vertical components of the magnetic field at each of the k measurement points in the measurement plane are calculated. These points, which are separated by 0.2 m, are located along a line 1 m above the terrain (see Fig. 1.a). The allocation of the measure plane 1 m above the terrain is frequently used in the literature, [1], [3], [8]-[13]. In the present simulations, k_{Max} is equal to 51, thus representing a measurement line of 10 m, 5 m to either side of the vertical axis. The square module of the magnetic field at all measurement points is restricted to the square of a specified maximum value, as in (4).

To determine the magnetic field at a point $P\ (X_c, Y_c)$ in the evaluation plane (Fig. 1.a) produced by the currents flowing through the wires of the circuit, the following assumptions are made [15]:

- The earth has no effect on the magnetic field produced by the cables ($\mu_r = 1$).
- The total magnetic field at any point is determined by a linear superposition of the magnetic field produced by the currents flowing through each individual conductor.
- The effect of induced shield currents on the magnetic field is negligible.
- Each cable is infinitely long and straight.
- Harmonic components can be neglected.
- The current flows through the centre of each conductor; the radius of the conductor is negligible with respect to the distance from the conductor to the evaluation plane.

ı the conductors points out of the page.

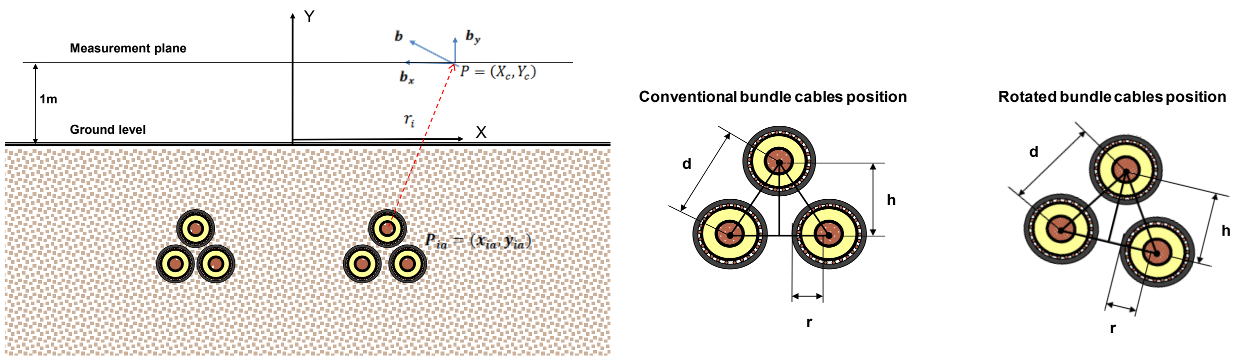

a *b* *c*

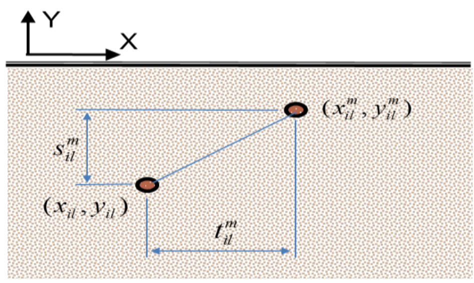

d

Fig. 1. *Geometrical diagrams.*
a Magnetic field generated by a conductor at point k.
b Conventional bundle cable
c Rotated bundle cable.
d Coordinates of the position for a mean arrangement and a sample m.

The centres of the cables in each bundle must be located on the vertices of an equilateral triangle, as specified in (5)-(7). In the present formulation, bundles can be rotated from conventional bundle cable positions (the two lowest cables at the same depth and the third placed above them, as in Fig. 1.b). Rotation of the bundles enables higher compensation and hence lower magnetic fields, [16], and this is obtained at negligible construction costs. Moreover, an approximation to near the conventional position can be used (Fig. 1.c) if rotated positions (Fig. 1.b) are not implemented in the installation of bundles.

The separation between cables in the same bundle is very important in the design of the circuit. A lower separation allows more compact solutions with lower construction costs. However, the ampacity of the bundle may be compromised by the inter-heating transfer among the cables in the bundle and the resulting limits on the allowed maximum current. Reductions in the separations between cables or circuits can require modifications in the section of the cables. Additionally, separation between the cables affects the interaction of the magnetic fields, as indicated by [6] and [8]. In the present study, the results of simulations using d = 0.32 m are presented; this value is based on the dimensions of the cables and in practical uses in Spain.

The coordinates of centres of the bundles i are calculated in (8)-(9). To guarantee that none of the 3-phase cable bundles overlap and to ensure sufficient distance between circuits (related to the desired ampacity), a minimum distance between circuits is imposed, as in (11). In the present simulations, the results correspond to d_{Min} = 0.8 m. Lower separation between cable bundles can also modify the ampacity of the circuits.

The depth of the trench (y_1) is defined by the deepest bundle. In (12), bundle i=1 is defined as the deepest bundle. For security reasons, Spanish legislation forbids the installation of wires at depths of less than 0.6 m. In addition, burial depths greater than 3 metres are beyond the capacity of usual construction equipment, and the maximum distance between two circuits is limited to 6 metres because of the nature of urban terrain, as in (13)-(14). Other external constraints, pipelines or obstacles can modify the characteristics of the parameters of the circuits [18] and the optimal results. In the proposed formulation, these geometrical constraints can be easily considered by the inclusion of additional equality and inequality restrictions in the optimization problem.

2.2. Calculation of mean coordinates for n cable bundles in M scenarios

The current in the cables varies during a day and depends on both the variations in the load and the dispatch of the grid. Magnetic fields interact with each other, thereby increasing or decreasing the values in the measurement plane. Therefore, the calculation of the optimal positions of the cable bundles must consider the possible variations in the currents. To calculate the optimal design based on a realistic situation, a simulation of alternative scenarios based on the distributions of current intensity is proposed, as presented in [17]. In the present study, real hourly data from 3 years of recording in underground installations are used to perform the statistical analyses. In contrast to [17], the distributions of the recorded currents were found to be non-normal. Furthermore, the empirical distributions show evidence of bimodality, mainly due to the presence of daily and weekly cycles. Trying to fit the data to some known distribution seems then a complex task. The proposed statistical approach is thus based on simulating the scenarios by resampling from the historical data. To this end, M samples, with replacement, of hourly current recordings conform to the scenarios of the study. For each of the scenarios, the optimization problem in (1)-(14) is solved, resulting in M optimal positions for the cable bundles.

The mean coordinates of the optimal arrangement of n 3-phase cable bundles can be calculated by obtaining the mean coordinates of the cables in the M scenarios satisfying geometrical constraints imposed on the bundles and cables. A second optimization problem is required here and is defined as follows:

$$min \quad h(x)=\sum_{m=1}^{M}\sum_{i=1}^{n}\left(\left(s_{ia}^{m}\right)^2+\left(s_{ib}^{m}\right)^2+\left(s_{ic}^{m}\right)^2+\left(t_{ia}^{m}\right)^2+\left(t_{ib}^{m}\right)^2+\left(t_{ic}^{m}\right)^2\right) \qquad (15)$$

s.t.

Eqs. (5)-(9) and (11).

$$x_{il}-s_{il}^{m}=x_{il}^{m} \qquad (16)$$

$$y_{il}-t_{il}^{m}=y_{il}^{m} \qquad (17)$$

Eqs. (13)-(14)

$i=1,\ldots,n$, $l=a,b,c$, $m=1,\ldots,M$.

where (x_{il},y_{il}) are the mean coordinates of cable l in the bundle of cables i of the optimal mean arrangement and s_{il}^{m},t_{il}^{m} are the horizontal and vertical distances from (x_{il},y_{il}) to each of the (x_{il}^{m},y_{il}^{m}) coordinates of the centres of cable l in the bundle of cables i for the m sample of currents. In the present optimization problem, (x_{il}^{m},y_{il}^{m}) are fixed values calculated using optimization problem (1)-(14).

Objective function (15) is the sum of square differences between coordinates of the centres of cable l in the bundle of cables i of sample m to the coordinates of the centres of the cables of the optimal mean arrangement s_{il}^{m}, t_{il}^{m}. In total, (6 x n x M) terms constitute the objective function. In the present formulation, all the differences are equally penalized. However, some other solutions can be wanted, prioritizing: a) less costly positions, b) less magnetic field solutions, c) less deeper configurations, or any other relevant aspect of the design. (5)-(9) and (11) express the geometrical equality restrictions that cables and bundles must respect. Therefore, these equations are repeated here. (16) and (17) define the differences between coordinates of the centres of the cables from each of the samples of the optimal arrangements (s_{il}^{m}, t_{il}^{m}) and the coordinates of the centre of the cables of the optimal mean arrangement. In Fig. 1.d, these variables are presented geometrically.

In (13) and (14), the normative and construction inequality restrictions for the centres of the bundles are shown. Therefore, these equations are also included in the optimal calculation of the mean position of the bundles.

3. Case study

In this section, a real-world case is analysed. The problem is the optimal connection of four underground power circuits of single-core XLPE cables, which use copper conductor with a 2,500 mm² cross-section. In this case, these real circuits are working at 220kV but the results of the analysis are suitable to circuits with the same currents and conductors at lower voltage. Also, the method can be used for any other configuration. The cables are bundled in a trefoil configuration, are directly buried and share a common path in the proximity of a substation, where they are all are connected. Two of the circuits end at other substation (Circuits 1 and 2) and the other two (Circuits 3 and 4) go to another substation, following partially divergent paths. Here, the initial sector with the four circuits in the same path is studied. The instantaneous values of active and reactive powers flowing through the four circuits have been recorded every hour for three years, generating a total of 24×365×3=26,280 registers. From these values, the active and reactive currents, $I = (I_d + \text{j}\, I_q)$, represented in Figs. 2.a and 2.b, are calculated.

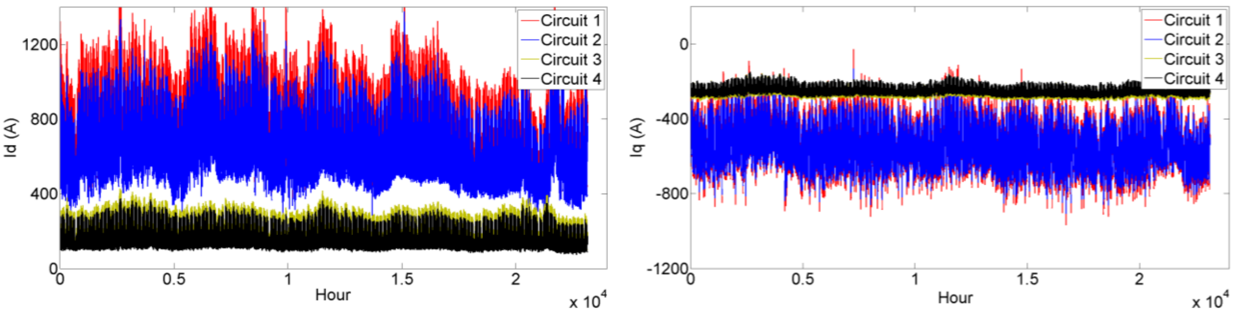

a *b*

Fig. 2. *Active currents of the four circuits.*

a I_d (A).
b I_q (A).

Demand, generation and even topology in power systems change continuously but usually follow certain seasonal patterns depending on the hour of the day, the day of the week and the season. Therefore, currents flowing through circuits vary over time but follow relatively similar patterns. Figs. 3.a and 3.b provide a sample of four weeks of data for active and reactive currents I_d and I_q.

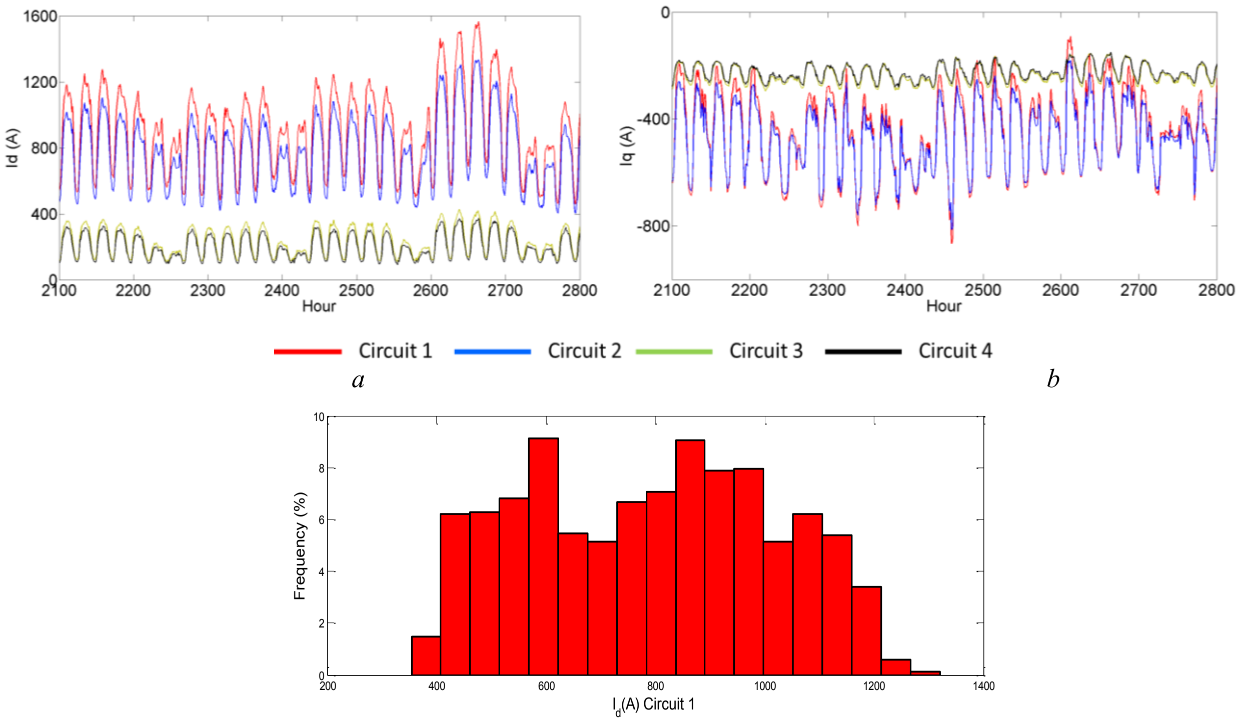

c

Fig. 3. *Sample of current contributing active power.*
a I_d (A), four first weeks.
b I_q(A), four first weeks.
c Histogram of I_d (A) in Circuit 1.

In Figs. 3.a and 3.b, a stochastic seasonal evolution of currents over the course of a day and between days in a week can be observed. The currents in Circuits 3 and 4 follow very similar profiles, whereas somewhat larger differences can be observed between Circuits 1 and 2. These figures also reveal an important fact: the statistical properties of the time series of currents are stable across time, i.e., there are not increasing or decreasing trends, and the seasonal (stochastic) patterns are maintained over time. Thus, it can be concluded that the unconditional distributions of the currents are stable. Hence, resampling from these distributions can provide a representative sample of the system. Then, the simulation of the behaviour of the whole configuration is performed by resampling from the unconditional distribution of the vector of currents. By doing so, it is possible to not only reproduce the univariate distribution of each current, which is not normal, but also preserve the interdependence between the currents. As an example, Fig. 3.c shows the histogram of I_d in Circuit 1. The histogram shows that the distribution is not normal; the distribution presents a multimodality that is due to its cyclic behaviour. The distributions of the remaining variables exhibit similar patterns.

To perform the statistical simulations, a random sample of size M = 150 time instants, from the available span of time, is selected. For each time instant, the corresponding vector of currents shown in Figs. 2.a and 2.b is obtained. The optimization problem (1)-(14) is solved for each of these 150 scenarios. In these simulations, the utilized values of the costs per unit are obtained from a general reference for construction costs in Andalusia, a southern region in Spain: c_x = 10 €/m², c_y= 14.59 €/m² and c_{vol} = 6.5 €/m³ [19]. In (1), only construction costs are considered; the costs of the cables themselves are not included. The penalty factor in the fourth term of (5) is (Kp=0.05·c_{vol}), therein prioritizing the cost reduction objective and, after that, the reduction in maximum magnetic fields (only if the minimum cost position is reached). For the geometrical constraints (13) and (14), which are related to the centres of the bundles, the values of X_{Max}=2.765 m, Y_{Min}=-0.835 m and Y_{Max}=-2.765 m are used.

4. Results

The proposed methodology is implemented and compared with more traditional solutions: the conventional position of bundles without rotation and a unique deterministic calculation with the maximum values of the currents. In total, six optimal configurations are compared. They are labelled as follows:

- *Med*: This configuration is based on the proposed statistical method. From historical data, M = 150 scenarios of instantaneous currents are randomly sorted. In each scenario, the optimization problem given in (1)-(14) is solved. Then, the mean arrangement of cables is calculated following the procedure described in Section 2.2.
- *MedStandard:* The *Med* configuration can utilize the benefits of rotated positions (as shown in Fig. 1.c). From this rotated configuration, *MedStandard*, the closest conventional bundle cable positions without rotation (as in Fig. 1.b) to the *Med* arrangement, is obtained.
- *Max:* This configuration is also based on the proposed statistical method. From the 150 solutions corresponding to the simulated scenarios specified for the *Med* configuration calculation, *Max* is the configuration of the optimal position with the maximum cost. This configuration can be viewed as the worst-case combination of currents.
- *MaxStandard:* This configuration represents the closest conventional bundle cable positions (as in Fig. 1.b), obtained from the *Max* configuration.
- *Det*: *Det* is the deterministic calculation of the optimal configuration, obtained by solving optimization problem (1)-(14) once, with fixed values in all circuits. As observed in Fig. 3, two circuits (1 and 2) have similar high currents and other two (3 and 4) are relatively less charged in all the hours. To reproduce this behaviour, in the first two circuits the maximum thermal current (1700 A) is considered and in the other two 360 A (the maximum current recorded in them) is assumed. The power factor is 0.8i in all cables. This configuration with fixed values in the cables is similar to the situations studied in most of the literature [8]-[16].
- *DetStandard:* The closest conventional (without rotation, as in Fig. 1.b) bundle cable positions of *Det*.

Different limits are specified for the maximum magnetic field across the world. To observe restrictive limits can be very difficult in many situations. The optimization method proposed in this work attempts to calculate the optimal positions of the underground cables under these restrictive conditions. Three cases are presented:

- B_{max} = *10 μT*. For values larger than 10 μT for the maximum magnetic field in the measurement plane, the minimum cost position can be reached for almost all the currents considered in the *Med*, *Max* and *Det* configurations. Therefore, when solving optimization problem (1)-(14) for B_{max} = 10 μT, the main objective is to search the optimal positions of cables generating the lowest maximum magnetic field at the minimum cost positions while meeting the geometrical constraints.
- B_{max} = *3 μT*. In general, this value of the maximum magnetic field requires configurations with costs that are larger than the minimum.
- B_{max} = *1 μT*. Most constringent condition here studied.

The three cases are presented below. Later, a cost comparison between configurations is performed.

4.1. B_{max} = 10 μT.

With B_{max} = 10 μT, all configurations are calculated and they share the same centres of the cable bundles. Therefore, they have the same construction costs, i.e., 36.70 €/m, the minimum allowed by the geometrical constraints. Circuits 1 and 2 are allocated to the two central positions, and Circuits 3 and 4 (with smaller currents) are moved to external points. However, the positions of the cables of the phases in each configuration are different, as depicted in Fig. 4.a. In all 150 sorted scenarios, the minimum cost position is obtained. Therefore, the *Max* and *MaxStandard* configurations are not applicable and are not represented in this case.

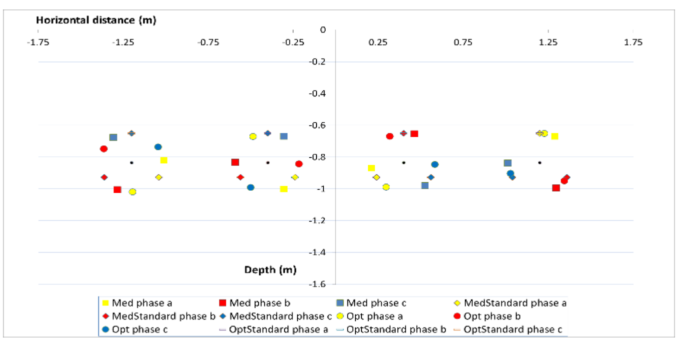

a

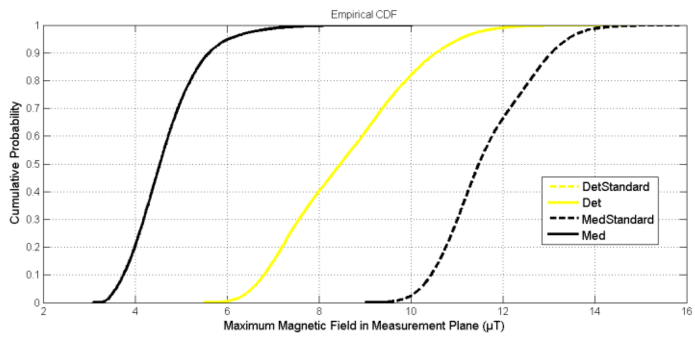

b

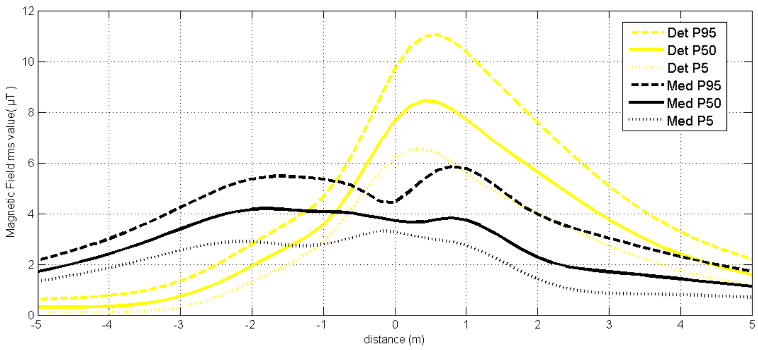

c

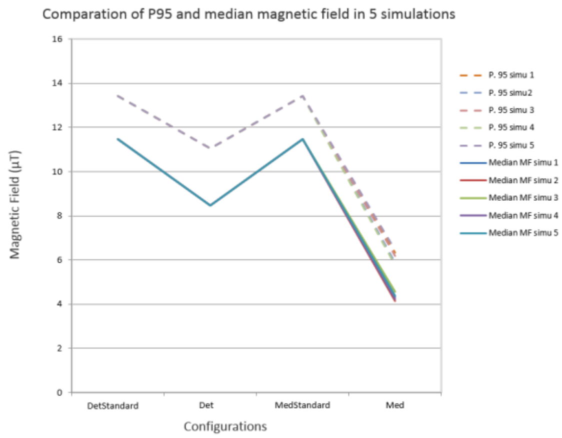

d

Fig. 4 *Results for* B_{max} *= 10 μT.*
a Positions of cables for four configurations.
b Empirical cdf of maximum magnetic field for four configurations.
c Percentiles of the Maximum Magnetic Field under the Det and Med Configurations.
d Comparison of P. 95 and Median Magnetic Field in five simulations.

All the hourly recorded values of Figs. 2.a and 2.b are applied to the *Med*, *MedStandard*, *Det* and *DetStandard* configurations of Fig. 4.a. In Fig. 4.b, the respective empirical cumulative distribution functions (cdfs) are depicted, therein providing statistical values of the probability of maximum magnetic field generated in the measurement plane. *Med* provides the best configuration, with maximum magnetic fields lower than 10.03 μT for all combinations of currents presented in the historical data. The advantages of the rotated positions are also observed in the figure. *MedStandard* and *DetStandard* share the same positions of cables and therefore provide the same empirical cumulative distribution function. *Med* and *Det* configurations produce smaller magnetic fields than do the *MedStandard* and *DetStandard* configurations, respectively, for all the historical data.

In Table 1, the median and 5th and 95th percentiles of all the hourly recorded values for the four configurations are presented. The median values of the *Det* and *Standard* (*Med* and *Det*) configurations are 86.15% and 152.31% larger than the *Med* configuration mean, respectively. Considering the 95th percentile, the magnetic field produced by the *Med* configuration is lower than 6.04 μT 95% of the time and *Det* and *Standard* (*Med* and *Det*) configurations are 83.11% and 122.18% larger than the *Med* configuration. As observed in Fig. 4.b and Table 1, the *Med* configuration has nearly a vertical distribution, with a small dispersion in the values. The almost flat distribution of the magnetic fields under the *Med* configuration can also be observed in Fig. 4.c, where some percentile levels of magnetic fields generated in all three years of hourly recorded values in the measurement plane are shown.

Table 1 B_{max} = 10 µT, some values of the cdfs.

Configuration	Magnetic field value (µT)		
	5th Percentile	Median	95th Percentile
DetStandard	10.20	11.48	13.42
Det	6.55	8.47	11.06
MedStandard	10.20	11.48	13.42
Med	3.58	4.55	6.04

To analyse the influence of the sample size in the *Med* and *MedStandard* calculations, five different sets of 150 values are used to calculate these configurations. In Fig. 4.d, the median and 95th percentile of the maximum magnetic field for the configurations in the five sets are depicted. As observed, the differences are negligible.

4.2. B_{max} = 3 µT.

With B_{max} = 3 µT, the six previously described configurations are calculated. In general, the centres of the cable bundles are positioned deeper than the minimum cost position in all simulations. Fig. 5 shows the empirical cdf of the maximum magnetic field in the six configurations. In Table 2, the median, the 5th and 95th percentiles and the cost of the six configurations are presented. The installation cost of the *Med* configuration is 39.40 €/m, 7.36% more expensive than the minimum cost. The average positions calculated in the *Med* configuration work very well with the historical data, resulting in a median value of 3.43 µT and a 95th percentile of 5.08 µT for the three recorded years. That is, the magnetic field is larger than 5.08 µT only 5% of the time at certain positions of the measurement plane. *Max* configuration is 20.43% more expensive than *Med* and, basically, as effective as this configuration when looking at median values (5% of reduction). However, *Max* configuration is more effective than *Med* when observing 95th percentile values, with a reduction of 14.37%.

In this case, the deterministic calculation performed using the *Det* configuration is the most ineffective method. As previously said, *Det* configuration is obtained by solving the optimization problem (1)-(14) once, with B_{max} = 3 µT and two circuits with the maximum thermal currents (1700 A) and in the other two circuits with 360 A. When applying the historical data to this configuration, the median value is 4.92 µT, namely, 43.44% larger than that in the *Med* configuration–and 50.09% larger than that in the *Max* configuration. *Det* configuration is also less efficient looking to 95th percentile values, resulting 45.52% and

24.61% higher than *Max* and *Med* configurations. Moreover, the cost of the *Det* configuration is 38.45% and 14.96% larger than the cost of *Med* and *Max* configurations, respectively.

To analyse the influence of the sample size under the *Med* and *Max* configurations, another five different sets of 150 values are used. Again, under different positions of the bundles, the median and maximum magnetic field generated by the *Med* configuration are negligible.

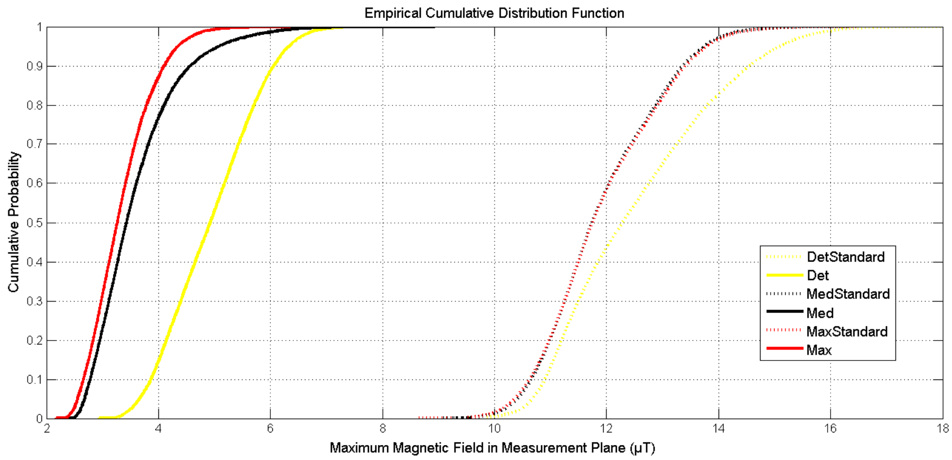

Fig. 5. *B_{max} = 3 µT, Empirical cdf of Maximum Magnetic Field for Six Configurations.*

Table 2 B_{max} = 3 µT, some values of the cdfs.

Configuration	Magnetic field value (µT) 5th Percentile	Median	95th Percentile	Cost (€/m)
DetStandard	15.01	12.28	10.68	54.55
Det	3.66	4.92	6.33	54.55
MedStandard	10.41	11.742	13.75	39.40
Med	2.68	3.43	5.08	39.40
MaxStandard	10.36	11.75	13.08	47.45
Max	2.56	3.26	4.35	47.45

4.3. B_{max} = 1 µT.

The calculation of the low cost positions of cables for very low magnetic fields and time-varying currents is a very difficult task. In the present study, the six configurations are calculated for B_{max} = 1 µT. With this target, the number of scenarios used to calculate *Med* and *Max* configurations can severely impact the results. For this, 750 samples of currents are used.

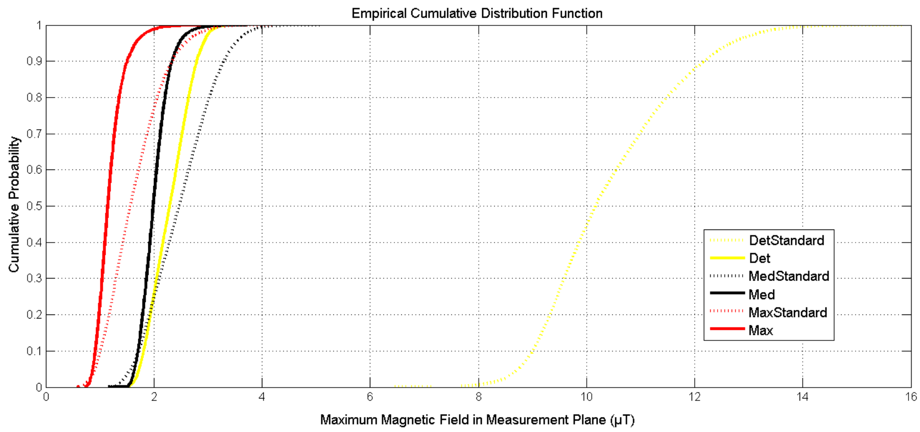

a

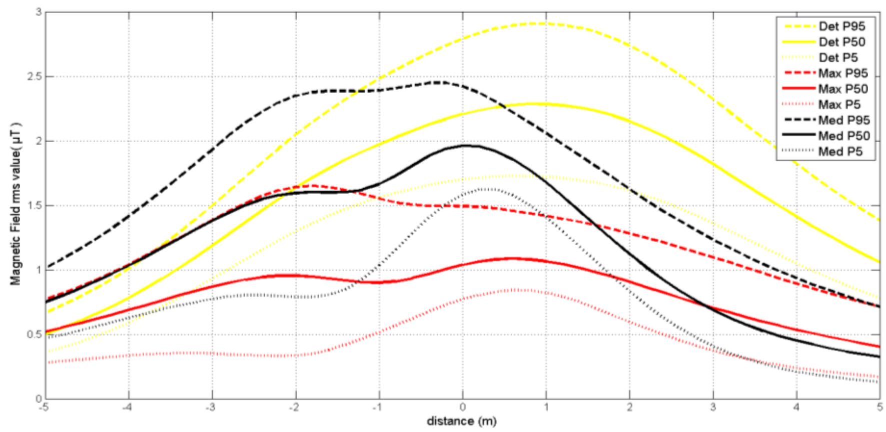

b

Fig. 6. *B_{max} = 1 μT, results.*
a Empirical cdf of Magnetic Field for Six Configurations.
b Percentiles of Magnetic Field in Measurement Plane.

In Fig. 6.a and Table 3, the empirical cdf, the median, the 5th and 95th percentiles for the six configurations are presented. *Med* configuration has a median value of 1.98 μT and *Max* of 1.15 μT, when applied across all historical data. These values are larger than the objective (1 μT) due to the variations in the modules and angles of the currents in all the recorded data, however they are very close to the specified limit. If considering the 95th percentile, deviations of magnetic field are relatively larger, 2.46 and 1.66, respectively. *Max* configuration is closer to the proposed objective than *Med* configuration, with a cost 27.89% higher. *Max* configuration seems to be more adequate for extremely reduced objectives of magnetic fields. In these cases, adopting more expensive configurations (even calculating with B_{max} < 1 μT) could be convenient, however increasing the installation costs.

From Table 3, *DetStandard* configuration has a 95th percentile value of 12.68 µT, the largest value of the six configurations, with costs 49.34% and 16.78% higher than *Med* and *Max* configurations, respectively. *Det* configuration, with the same high cost, has worse magnetic field values than *Med* and *Max* configurations.

Table 3 B_{max} = 1 µT, some values of the cdfs.

Configuration	Magnetic field value (µT) 5 Percentile	Median	95 Percentile	Cost (€/m)
DetStandard	8.74	10.16	12.68	93.28
Det	1.73	2.29	2.91	93.28
MedStandard	1.57	2.46	3.51	62.46
Med	1.64	1.98	2.46	62.46
MaxStandard	0.91	1.56	2.57	79.88
Max	0.86	1.15	1.66	79.88

In Fig. 6.b, the distributions of median values, 5th and 95th percentiles in the measurement plane are presented. Asymmetric magnetic fields can be observed in the curves, due to imbalances in the real currents of the circuits.

4.4. Cost Comparisons

In Fig. 7, the median and 95% percentile of the maximum magnetic field for *Max*, *Med* and *Det* configurations are presented, as a function of the installation cost. To obtain maximum magnetic fields larger than B_{max} = 5 µT, *Med* configuration requires lower installation costs, according to the curve of mean and 95% percentile values of the magnetic fields. However, for stronger magnetic field constraints (B_{max} < 5 µT), the *Max* configuration seems to be preferable.

Below 5 µT, standard and rotated curves for *Med* and *Max* configurations are quite parallels. However, the ramp of the curves is steep. Therefore, the economic difference on considering the same maximum magnetic field in median and 95% percentile is considerable. As an example, for a maximum magnetic field of 2.4 µT and *Max* configuration, the increment in the construction cost between median and 95% percentile curves is 29.63%, from 55 to 71.3 €/m.

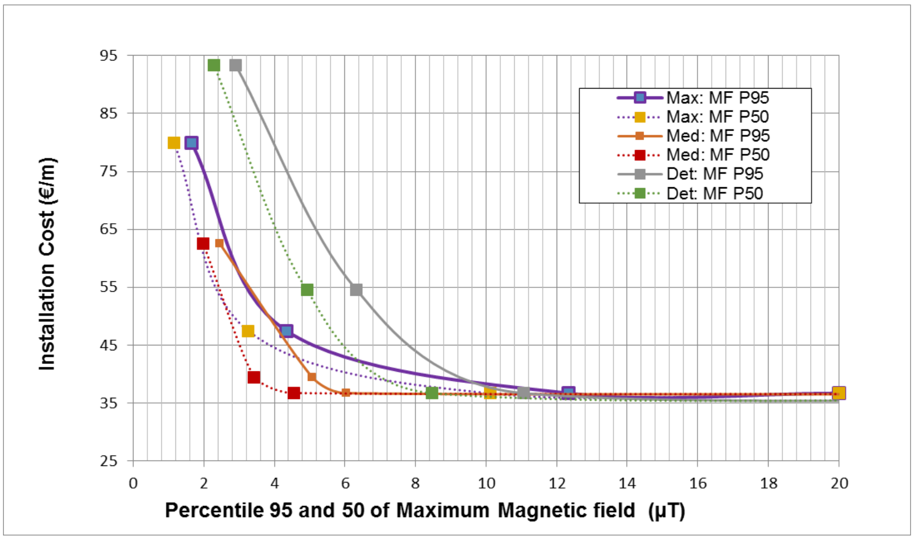

Fig. 7. *Mean and 95th Percentile curves vs. installation cost.*

The optimization problems proposed in this paper can be applicable to different cable configurations, geometrical restrictions and normative. However, the solutions can be different, in function of the configuration of the terrain and characteristics of local normative. As an example, the sensitivity of solutions as a function of the height of measure plane is presented here. The magnetic field restricted by normative, [1]-[5] , is usually considered in an evaluation plane 1 m above the terrain. However, some other heights of the evaluation plane can be considered. In Fig. 8, installation costs for different heights of the evaluation plane are depicted, for $B_{max}=3\mu T$. The two statistical configurations (*Max* and *Med*) are compared with the conventional solution *Det*. Up to a height of 1.3 m, the most expensive configurations are *Det* and *Max*, in this order, keeping a constant cost difference with *Med*. For the measure plane at approximately 1.5 m high, the three configurations reach minimum cost positions; therefore, larger heights of the measure plane cannot reduce the installation cost. It must be stressed that *Med* configuration reaches the minimum cost position for a measure plant slightly above 1 m, 50% before the other two configurations.

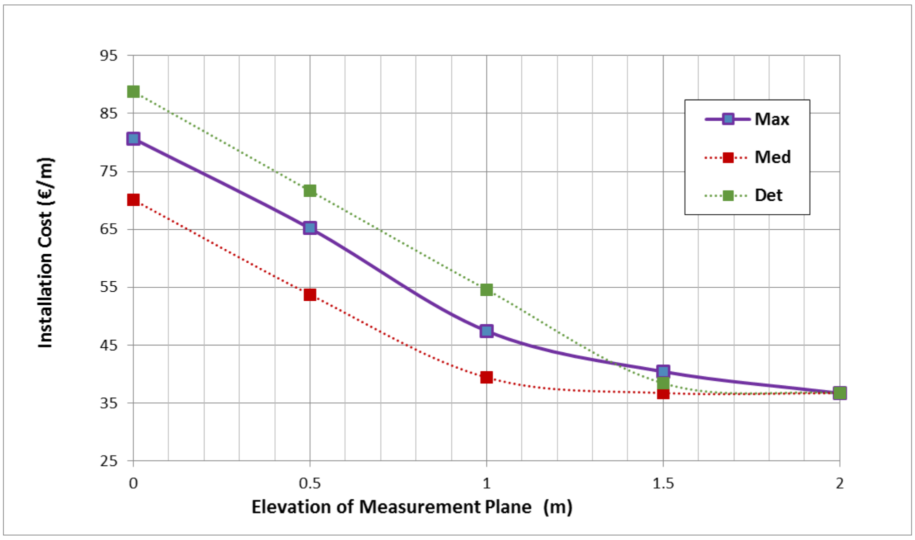

Fig. 8. *Height of Measurement Plane vs. Installation Cost, Bmax=3 µT.*

5. Conclusions

This work proposes and compares methods for optimizing the allocation of *n* bundles of cables with time-varying currents through them, therein considering maximum magnetic field, geometrical constraints and installation cost. A real-world case with four cable bundles and three years of historical data is analysed. Two statistical configurations, namely, the worst-case combination of currents and the mean calculation, are compared with the usual deterministic calculation method. Additionally, benefits due to the rotated positions of cables are determined.

In the case study, the proposed statistical approach is found to be far more convenient than the traditional deterministic method. The deterministic method can be up to 50% more costly and can produce magnetic fields that are 390% larger than those of the statistical methods. The rotation of bundles provides also great reductions in the magnetic fields.

From the results with real currents flowing in the cables, installation costs are different when considering the magnetic field limit in different quantiles. Therefore, normative must be explicit about which quantile must be considered for the restriction, for cables with time-variants currents.

References

[1] International Commission on Non-Ionizing Radiation Protection, Guidelines for Limiting Exposure to Time Varying Electric and Magnetic Fields (Up To 100 kHz). ICNIRP Guidelines: 2010.

[2] Limits in the USA. EMFS, available online: http://www.emfs.info/, last visit: Jan. 2016.

[3] European Commission. Council Recommendation of 12 July 1999 on the Limitation of Exposure of the General Public to Electromagnetic Fields (0 Hz to 300 GHz), The Council of The European Union: 1999.

[4] Rianne Stam (Laboratory for Radiation Research, National Institute for Public Health and the Environment, the Netherlands). Comparison of International Policies on Electromagnetic Fields (Power Frequency and Radiofrequency Fields): May 2011.

[5] European Commission. Report on the implementation of the Council Recommendation on the limitation of exposure of the general public to electromagnetic fields (0 Hz – 300 GHz) (1999/519/EC) in the EU Member States, Commission staff working paper: 2008.

[6] CIGRE Working Group C4.204. Mitigation Techniques of Power Frequency Magnetic Fields Originated from Electric Power Systems: Feb. 2009.

[7] Muñoz, F., et al. An intelligent computing technique to estimate the magnetic field generated by overhead transmission lines using a hybrid GA-Sx algorithm. International Journal of Electrical Power & Energy Systems 53 (2013): 43-53

[8] Karady, G. G., Nunez, C. V., Raghavan, R. The Feasibility of Magnetic Field Reduction by Phase Relationship Optimization in Cable Systems. IEEE Transactions on Power Delivery 13(2): April 1998.

[9] Mimos, E. I., Tsanakas, D. K., Tzinevrakis, A. E. Optimum phase configurations for the minimization of the magnetic fields of underground cables. Electrical Engineering 91(6): 327-335: 2010.

[10] Yang, C. F., Lai, G. G., Su, C. T., Huang, H. M. Mitigation of magnetic field using three-phase four-wire twisted cables. Int. Trans. Electr. Energ. Syst. 23: 13–23: 2013.

[11] Canova, A., Bavastro, D., Freschi, F., Giaccone, L., Repetto, M. Magnetic shielding solutions for the junction zone of high voltage underground power lines. Electric Power Systems Research 89: 109–115: 2012.

[12] Pino-López, J.C. del, Cruz-Romero, P., Serrano-Iribarnegaray, L., Martínez-Román, J. Magnetic field shielding optimization in underground power cable duct banks. Electric Power Systems Research 114: 21–27: 2014.

[13] Ippolito, M. G., Puccio, A., Ala, G., Ganci, S. Attenuation of low frequency magnetic fields produced by HV underground power cables. Power Engineering Conference (UPEC 2015) 50th International Universities: 1-5: 2015.

[14] Jiang, Yi-Hsuan, Wu-Chung Su, and Ming-Yen Wey. Numerical electromagnetic analysis of a junction tower with cable arrangements. International Journal of Electrical Power & Energy Systems 62 (2014): 103-109.

[15] Lai, G. G., Yang, C. F., Huang, H. M., Su, C. T. Optimal Connection of Power Transmission Lines with Underground Power Cables to Minimize Magnetic Flux Density Using Genetic Algorithms. IEEE Trans. on Power Delivery 23(3): 2008.

[16] Hernandez Jimenez, V. J., Castronuovo, E. D. Optimal geometric configurations for mitigation of magnetic fields of underground power lines. PowerTech, 2015 IEEE Eindhoven: 1-6: 2015.

[17] Lai, G. G., Yang, C., Su, C. Estimation and management of magnetic flux density produced by underground cables in multiple-circuit feeders. European Transactions on Electrical Power 20 (2010): 545–558: 2010.

[18] Wu, Xuan, Hui Zhang, and George G. Karady. Transient analysis of inductive induced voltage between power line and nearby pipeline. International Journal of Electrical Power & Energy Systems 84 (2017): 47-54.

[19] Table of prices of the construction in Andalusia (Base de Costes de la Construcción de Andalucía (BCCA) 2013. Banco de Precios): 2016 (in Spanish). Available online http://www.juntadeandalucia.es.